Pyrophoric Films Based on Nano-Sized Iron

Zac Doorenbos[1], Alok Vats[1], Jan Puszynski[1], Rajesh Shende[1], Deepak Kapoor[2], Darold Martin[2], Chris Haines[2]

[1]Department of Chemical and Biological Engineering, South Dakota School of Mines and Technology, Rapid City, SD

[2]Armament Research, Development, and Engineering Center, Picatinny, NJ

Abstract

Pyrophoric α-iron nanostructured porous coatings were prepared using a sol-gel technique. Iron oxide coating deposited on a non-porous metallic substrate was formed from $FeCl_2 \cdot 2H_2O$ dissolved in ethanol in the presence of Brij-76 or Pluronic P123 surfactant. The gelling process was conducted by the addition of propylene oxide. The surfactant was removed, in some experiments, by washing in ethanol and the resulting coating was heat treated to form Fe_2O_3. The Fe_2O_3 coatings were reduced in H_2/N_2 atmosphere at temperatures above 500°C and after cooling tested for their pyrophoricity in air. These coatings have shown a strong affinity to oxygen. The effect of processing conditions as well as thickness of the coating and it morphology on maximum combustion temperature and the duration of the pyrophoric reaction will be discussed. Experimental data will be compared to results obtained from one-dimensional mathematical model.

Introduction

The use of pyrophoric materials in everyday applications is important in both the military and commercial applications. Its uses range from the protection of aircraft to hand and muscles warmers. One area that has had a great deal of focus lately is the use of pyrophoric materials for infrared countermeasures for aircraft.

Of the several different pyrophoric materials that could be used, iron (Fe) in the form of fine particles is highly reactive and pyrophoric [1] and has not received as much attention as the others. Fe nano particles have found a great deal of interest for their use in non-pyrophoric applications such as catalysis [2], magnetic resonance imaging [3], magnetic data storage [4], coatings [5], synthesis of carbon nanotubes [6], synthesis of highly oriented and ordered nanostructures for field emission devices [7] etc. Previously, Gash et al. [8] and Shende et al. [9,10] have published work showing Fe based foils with a pyrophoric response when exposed to air. The work done by Gash et al. was based on a sol-gel technique using a precursors of $Fe(NO_3)_3.9H_2O$, $F_2Cl_3.6H_2O$, or anhydrous $FeCl_3$. The gels were subsequently reduced in H_2 and H_2/Ar environments at temperatures ranging from 350-700°C. The films did not show a pyrophoric response when exposed to air. However, once thermally ignited the films were self-sustaining. Gash et al. suggested that the addition of another metal would aid in the pyrophoric response of the Fe films. Shende et al. showed that it was possible to generate a pyrophoric response from iron obtained by thermal decomposition and reduction of Fe-oxalate/yttria films [9]. The Fe-oxalate/yttria films were made by dip coating a thin stainless steel substrate with a

mixture of yttria sol-gel and Fe-oxalate using different weight ratios of starting precursors. The Fe-oxalate films showed a pyrophoric temperature response over 800^{o}C.

Very little previous work has been done on the mathematical modeling of combustion front propagation in foils when exposed to air. In the paper written by Wilharm [11] a mathematical model that predicts the pyrophoric response of Fe based foils when exposed to air was proposed. Because of the small pore diameter in porous iron foils it is assumed that the diffusion of the oxygen is the rate limiting step of the reaction. The author reports the results of the mathematical model but does not compare modeling results to any experimental data. Wilharm [11] concludes that the foils characteristics are dependent on "The pore diameter, specific surface area, and porosity…". The foil characteristics, as mentioned by Wilharm, are dependent on the production method and substrate use for foil generation.

Experimental

The goal of this research was to generate a pyrophoric foil that will generate a pyrophoric response of greater than 800^{o}C in less than 1 second. It is also important that the film adheres to the substrate and that the process of making the films is cheap and non-labor intensive. The first method which uses Fe-oxalate films as was reported by Shende et al. [9], is a labor intensive and time consuming process. A better way of generating these films would be to use a one step Fe_2O_3 sol-gel based process and spin or dip coating of the substrate with a sol-gel.

To accomplish this task the following raw materials were used: $FeCl_2{\cdot}2H_2O$ powder (Alfa Aesar), absolute ethanol (Sigma Aldrich), propylene oxide (PO)(Sigma Aldrich Reagent Grade), Pluronic P123 Surfactant (BASF), Brij-76 Surfactant (Sigma Aldrich), stainless steel foil and alumina felt (McMaster Carr).

The generation of the sol-gel was done using the following steps: 1) Addition of the $FeCl_2{\cdot}2H_2O$ to the absolute ethanol, 2) The addition of the surfactant (if being used), 3) Sonication to dissolve $FeCl_2{\cdot}2H_2O$ and surfactant, 4) addition of PO and mixing. After these steps are completed the gel was formed in 1 to 9 minutes, depending on the amount of PO added. The sol-gel was coated onto the stainless steel substrate by spin coating at 80% of its total gel time. When a porous substrate was used instead, a dip coating was applied at 80% of its total gel time. The substrates were then calcined in air at a heating rate of 0.5^{o}C up to 400^{o}C and allowed to cool to room temperature. The samples were then reduced in a H_2 atmosphere at 500^{o}C for 10-20 minutes. The reduction time is dependent on the amount of Fe_2O_3 that is present in the initial sample. The foils were then exposed to air and their pyrophoric temperature responses are recorded using a Fluke IR pyrometer. Photographs of the FeOOH sol-gels coated onto the two different substrates are shown in Figure 1.

Figure 1: *a) Sol-gel coating on stainless steel substrate after calcination, b) sol-gel coating on porous alumina substrate after calcination.*

Results

The FeOOH sol-gel is converted to Fe_2O_3 after calcination. When the Fe_2O_3 is reduced in a H_2 environment results in the formation of α-Fe. This α-Fe is pyrophoric when exposed to air. The pyrophoric temperature profiles generated when the α-Fe is in powder form, coated on stainless steel and coated onto a porous substrate when exposed to air are shown in Figure 2.

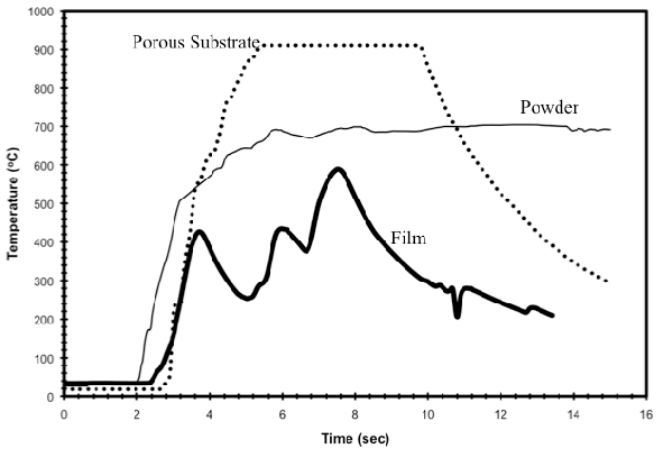

Figure 2: *Pyrophoric temperature response of sol-gel based α-Fe powder, Fe based film coated on stainless steel, and Fe coated porous substrate.*

The pyrophoric responses shown in Figure 2 indicate that the porous substrate has the best pyrophoric response reaching a temperature of over 900°C. The use of a porous substrate allows for an increase in surface area allowing for more Fe to present in the foil and oxygen to diffuse from both sides of the foil.

To investigate the surface morphology of the α-Fe after reduction a small amount of oxygen was introduced into the furnace, for one sample, passivating the iron allowing for it to be exposed to air without burning. A SEM image of the porous substrate coated with passivated Fe is shown in Figure 3.

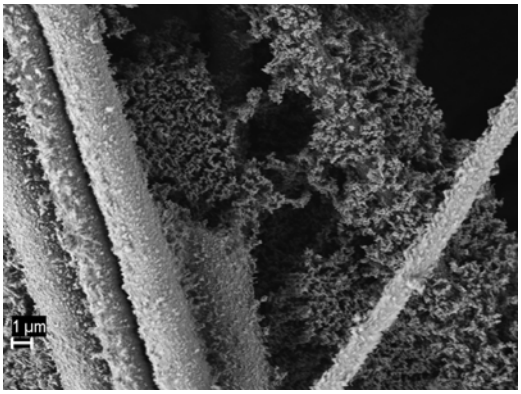

Figure 3: *SEM of the porous alumina substrate coated with passivated iron from the FeOOH sol-gel.*

In the experimental section it was mentioned that a surfactant can be added to the sol-gel. In theory this would increase the surface area of the material formed. Surface area analysis was done using BET. The Fe_2O_3 after calcination actually decreased with increased surfactant concentration. The use of a surfactant did not appear to have an effect on either the rise time or the maximum temperature that could be achieved but instead had an effect on the time length at which the foil burned at its maximum temperature.

In order to obtain a better understanding of the burning characteristics and be able to predict the pyrophoric response when exposed to air a mathematical model has been proposed. It was assumed for the initial model that the Fe foil could be modeled using the particle-pellet model for a gas solid reaction. Sampath et al. [12] proposed the particle-pellet model for the following reaction:

$$A_{(g)} + bB_{(s)} \longrightarrow \text{Products}$$

The use of this type of model would allow for the modeling of either diffusion controlled or reaction controlled reactions. Using Sampath's approach and the kinetic data data from Grosvenor et al. [12] the following mathematical model was derived. When modeling this system there are three equations that must be considered: 1) mass transfer of oxygen into the foil, 2) heat transfer from the reacting foil to the surroundings, and 3) the kinetic equation for the oxidation reaction. The key model equations are shown below (Eqs 1-3) and a schematic of the foil that is being modeled is shown in Figure 4.

$$D_{eff}\frac{\partial^2 C_A}{\partial x^2} - (-r_A) = \varepsilon_2 \frac{\partial C_A}{\partial t} \tag{1}$$

$$k_{eff}\frac{\partial^2 T}{\partial x^2} + (-\Delta H)(-r_A) = \left[(1-\varepsilon_1-\varepsilon_2)\rho_{Fe}C_{p_{Fe}} + \varepsilon_1\rho_i C_{p_i} + \varepsilon_2\rho_g C_{p_g}\right]\frac{\partial T}{\partial t} \tag{2}$$

$$-\frac{dr_c}{dt} = AR^{0.6}T^{0.6}C_A^{0.6}e^{-E/RT}e^{-\gamma(r_0-r_c)/RT} \tag{3}$$

Figure 4: *Schematic of Fe foil for the mathematical model.*

The model equations were converted to a dimensionless form for numerical convience. The dimensionless equations are shown below (Eqs 4-6). The equations were derived with the assumption that diffusion inside a porous structure is the rate limiting step. Knudsen diffusion was considered in this case only.

$$\frac{\partial^2 Y_A}{\partial \xi^2} - K_2 Z^2 \Theta^{0.6} Y_A^{0.6} e^{\frac{-(\beta_1+\beta_2(1-Z))}{\Theta}} = K_1 \frac{\partial Y_A}{\partial \tau} \tag{4}$$

$$\frac{\partial^2 \Theta}{\partial \xi^2} + \Omega K_2 Z^2 \Theta^{0.6} Y_A^{0.6} e^{\frac{-(\beta_1+\beta_2(1-Z))}{\Theta}} = K_3 \frac{\partial \Theta}{\partial \tau} \tag{5}$$

$$\frac{\partial Z}{\partial \tau} = Y_A^{0.6} \Theta^{0.6} e^{\frac{-(\beta_1+\beta_2(1-Z))}{\Theta}} \tag{6}$$

$$\tau = t \,{}^{A}\!/_{r_0} R^{0.6} T_g^{0.6} C_{Ag}^{0.6} \tag{7}$$

The dimensionless constants listed in equations 4-6 are defined in equations 8-13.

$$K_1 = \frac{\varepsilon_2 L^2}{D_{eff}} \frac{A}{r_0} R^{0.6} T_g^{0.6} C_{Ag}^{0.6} \tag{8}$$

$$K_2 = \frac{L^2}{C_{Ag} D_{eff}} \frac{3A}{b} \frac{(1-\varepsilon_1-\varepsilon_2)}{r_0 M_{Fe}} \rho_{Fe} R^{0.6} T_g^{0.6} C_{Ag}^{0.6} \tag{9}$$

$$K_3 = \frac{\left[(1-\varepsilon_1-\varepsilon_2)\rho_{Fe} C_{p_{Fe}} + \varepsilon_1 \rho_i C_{p_i} + \varepsilon_2 \rho_g C_{p_g}\right] L^2}{k_{eff} r_0} A R^{0.6} T^{0.6} C_{Ag}^{0.6} \tag{10}$$

$$\Omega = \frac{D_{eff} C_{Ag} (-\Delta H)}{k_{eff} T_g} \tag{11}$$

$$\beta_1 = \frac{E}{R T_g} \tag{12}$$

$$\beta_2 = \frac{\gamma r_0}{RT_g} \tag{13}$$

The initial and boundary conditions are as follows:

Initial conditions:

t = 0

$$\frac{\partial \Theta}{\partial \xi} = 0 \tag{14}$$

$$\frac{\partial Y_A}{\partial \xi} = 0 \tag{15}$$

Boundary conditions:

x = 0

$$\frac{\partial Y_A}{\partial \xi} = 0 \tag{16}$$

$$\frac{\partial \Theta}{\partial \xi} = 0 \tag{17}$$

x = L

$$\frac{\partial Y_A}{\partial \xi} = Sh(1 - Y_A\big|_L) \tag{18}$$

$$\frac{\partial \Theta}{\partial \xi} = Nu(\Theta - 1) \tag{19}$$

This system of partial differential equations is presently being solved using FlexPDE computational software. The terms, ε_1 and ε_2 account for the SiO_2-Al_2O_3 substrate and iron porosity, respectively. The generation of pyrophoric foils using a Fe based sol-gel method has been shown and the mathematical model is currently being investigated.

Acknowledgements

The authors of this paper acknowledge the financial support by the Army Research Development Engineering Center in Picatinny Arsenal, NJ (Contract No. WI5QKN-06-D-0006).

Definition of Variables

A = pre-exponential factor for Arrhenius equation
B = stoichiometric coefficient of reaction
C_A = concentration of oxygen at any point, (mol/m^3)
C_{Ag} = concentration of oxygen in the bulk, (mol/m^3)
$C_{p,FE}$ = Specific heat capacity, (J/kg K)
$C_{p,g}$ = Specific heat capacity, (J/kg K)
$C_{p,i}$ = Specific heat capacity, (J/kg K)
D_{eff} = effective diffusivity, (m^2/s)
E = activation energy (kJ/mol)
k_{eff} = effect thermal conductivity, (W/m K)
Nu = Nusselt number
R = gas constant, (8.314 J/mol K)
r_c = radius at the reaction front, (nm)
r_o = radius of the particles, (nm)
Sh = Sherwood number
t = time, (sec)
T = Temperature at any point (K)
T_g = Temperature of the surrounding gas (K)
Y_A=dimensionless concentration , C_A/C_{Ag}
Z = dimensionless radius, r_c/r_o

Greek Symbols

ξ = dimensionless distance, x/L
ε_1 = porosity of the inert substrate
ε_2 = porosity of the iron
Θ = dimensionless temperature T/T_g
τ = dimensionless time
ρ_{Fe} = density of Fe, (m^3/kg)
ρ_g = density of gas, (m^3/kg)
ρ_i = density of inert substrate, (m^3/kg)
γ = increase in activation energy with respect to oxide layer, (kJ/mol nm)

References

[1] E.A. Shafranovsky, Yu. I. Petrov, "Aerosol Fe Nanoparticles with the Passivating Oxide Shell", Journal of Nanoparticle Research. 6, 1, 71-90, 2004.

[2] Xuanke Li, Zhongxing Lei, Rongcui Ren, Jing Liu, Xiaohua Zuo, Zhijun Dong, Houzhi Wang, Jianbo Wang, "Characterization of carbon nanohorn encapsulated Fe particles", Carbon, 41, 15, 3068-3072, 2003.

[3] Stefan G. Ruehm, Claire Corot; Peter Vogt, Stefan Kolb, Jörg F. Debatin, "Magnetic Resonance Imaging of Atherosclerotic Plaque With Ultrasmall Superparamagnetic Particles of Iron Oxide in Hyperlipidemic Rabbits" Circulation, 103 , 415-422, 2001.

[4] S. A. Majetich, Y. Jin, "Magnetization Directions of Individual Nanoparticles" Science, 284, 5413, 470 – 473, 1999.

[5] Satoshi Tomita, Masahiro Hikita, Minoru Fujii, Shinji Hayashi, Keiichi Yamamoto, "A new and simple method for thin graphitic coating of magnetic-metal nanoparticles", Chemical Physics Letters, 316(5-6),361-364, 2000

[6] Yoshikazu Homma, Takayuki Yamashita, Paul Finnie, Masato Tomita, Toshio Ogino, "Single-Walled Carbon Nanotube Growth on Silicon Substrates Using Nanoparticle Catalysts", Jpn. J. Appl. Phys., 41, L89-L91, 2002

[7] C. H. Liang, G. W. Meng, L. D. Zhang, Y. C. Wu, Z. Cui, "Large-scale synthesis of β-SiC nanowires by using mesoporous silica embedded with Fe nanoparticles", Chemical Physics Letters, 329, 3-4, 323-328, 2000.

[8] A.E. Gash, J.H. Satcher Jr., R.L. Simpson, "Preparation of porous pyrophoric iron using sol-gel method", US Patent 20060042412, Appl. No. 11/165734.

[9] R. V. Shende, A. Vats, Z.D. Doorenbos, D. Kapoor, D. Martin, J.A. Puszynski, "Formation of pyrophoric iron particles by H_2 reduction of oxalates and oxides", 7th International Symposium on Special Topics in Chemical Propulsion, Kyoto, Japan, Sep. 17-21, 2007 (to be published).

[10] Rajesh Shende, Alok Vats, Zac Doorenbos, Deepak Kapoor, Christopher Haines, Darold Martin, and Jan Puszynski, "Formation of Pyrophoric α-Fe Nanoparticles from Fe(II)-Oxalate," NSTI-Nanotech (ISBN 978-1-4200-8503), 1, 692, 2008.

[11] C.K. Wilharm, "Combustion Model for Pyrophoric Metals Foils", Propellants, Explosives, Pyrotechnics, 6, 28, 296-300, 2003.

[12] B.S. Sampath, P.A. Ramacandran, R. Hughes, "Modeling of Non-Catalytic Gas-Solid Reaction –I. Transient Analysis Of The Particle-Pellet Model", Chemical Engineering Science, 30, 125-134, 1975.

[13] A.P. Grosvenor, B.A. Kobe, N.S. McIntyre, "Activation Energies for Oxidation of Iron by Oxygen Gas and Water Vapour", Surface Science, 574, 317-321, 2005.